2018-08-01

Total Hemispherical Apparent Radiative Properties of the Infinite V-Groove with Diffuse Reflection

Rydge B. Mulford
Brigham Young University - Provo

Nathan S. Collins
Brigham Young University - Provo

Michael S. Farnsworth
Brigham Young University - Provo

Matthew R. Jones
Brigham Young University - Provo

Brian D. Iverson
Brigham Young University - Provo, bdiverson@byu.edu

Technical Notes

Total Hemispherical Apparent Radiative Properties of the Infinite V-Groove with Diffuse Reflection

Rydge B. Mulford,* Nathan S. Collins,†
Michael S. Farnsworth,* Matthew R. Jones,‡
and Brian D. Iverson§
Brigham Young University, Provo, Utah 84602

Nomenclature

A, B, C	=	V-groove surfaces for view factor relationships
A_p	=	opening area, m²
A_t	=	emitting area, m²
a	=	length of partially illuminated surface, m
D, E, G	=	correlation constants
F_{x-y}	=	view factor from surface x to surface y
N_a	=	number of rays absorbed by the cavity surfaces
N_e	=	number of rays that escape from the cavity opening
N_t	=	total number of rays present in the simulation
n	=	sample size
q_a	=	absorbed heat rate, W
q_e	=	escaped heat rate, W
q_t	=	total heat rate, W
s	=	sample standard deviation
α	=	intrinsic absorptivity of the material
α_a	=	apparent absorptivity of a cavity
γ	=	collimation angle of incident irradiation, rad
ε	=	intrinsic emissivity of the material
ε_a	=	apparent emissivity of a cavity
θ	=	polar angle of a ray, rad
$\Lambda_1, \Lambda_2, \Lambda_3$	=	correction functions
ρ_a	=	apparent reflectivity of a cavity
σ	=	Stefan–Boltzmann constant, W · m⁻² · K⁻⁴
ϕ	=	V-groove opening angle, rad

I. Introduction

DYNAMIC control of radiative surface properties enables optimization of thermal management systems for spacecraft, radiative cooling systems, and other applications [1–3]. Various methods of altering the absorption or emission from a surface have been investigated [4–6]. Use of origami-inspired tessellated surfaces to control apparent radiative surface properties is a promising technology [7–9]. Realizing the full potential of tessellated surfaces

to dynamically control apparent radiative surface properties requires convenient methods of calculating apparent properties as a function of tessellation geometry and intrinsic radiative surface properties. This Note focuses on the use of geometry to affect total, hemispherical properties of V grooves comprising diffuse, gray surfaces.

When radiant thermal energy enters a cavity, multiple reflections result in greater absorption than that of an equivalent flat surface. Likewise, multiple reflections concentrate radiation emitted from the cavity walls, which increases emission from the cavity above that of an equivalent flat surface. This behavior is termed the cavity effect, and it is quantified using apparent absorptivity and apparent emissivity.

The accordion tessellation is an ideal candidate for an origami-inspired variable emissivity device. A V-groove is easy to manufacture, and its geometry is changed with simple linear actuation. Models of the apparent radiative surface properties of V grooves were developed by Sparrow and Lin [10,11], as well as other models stemming from these initial publications [12–17]. These models are presented as nested integral equations that must be solved simultaneously.

This Note presents a series of correlations that allow rapid computation of apparent radiative properties of isothermal, diffusely reflecting, infinite V grooves that are exposed to diffuse and collimated irradiation. The case of specular reflection with collimated or diffuse irradiation is treated separately [18].

These correlations, which are based on extensive Monte Carlo simulations, give the apparent radiative properties as a function of cavity angle (ϕ as shown in Fig. 1a), intrinsic surface properties, and the collimation angle (γ as shown in Fig. 1a) where applicable. Presented as series solutions, these correlations are simpler to implement than the nested integral equations reported previously. Although the periodic structure of tessellated surfaces is similar to that of a diffraction grating, the length scale of a V-groove is orders of magnitude greater than wavelengths associated with thermal radiation. Therefore, the diffraction and effects associated with near-field radiative transfer are negligible [5,6,19].

II. Methodology

A. Monte Carlo Ray Tracing

Monte Carlo ray tracing [20–22] is a straightforward numerical method that may be used to quantify the apparent emissivity and apparent absorptivity of arbitrarily shaped cavities for diffuse reflection/emission and uniform radiative surface properties [23]. Applying the principle of conservation of energy to a cavity gives an expression for the apparent emissivity of the cavity. Because the ratio of escaped energy to emitted energy (q_e/q_t) is equal to the ratio of escaped rays to emitted rays (N_e/N_t), the apparent emissivity of the cavity is found through an energy balance, giving Eq. (1):

$$\varepsilon_a = \varepsilon \left(\frac{A_t}{A_P} \right) \left(\frac{N_e}{N_t} \right) \tag{1}$$

To obtain apparent absorptivity, a specified radiative heat rate, which is proportional to N_t, is emitted diffusely or at some collimation angle γ from the opening A_p into the cavity. After one or more interactions with the cavity walls, the radiant energy is either absorbed or reflected through the opening. Again, application of the conservation of energy gives an expression for the apparent absorptivity:

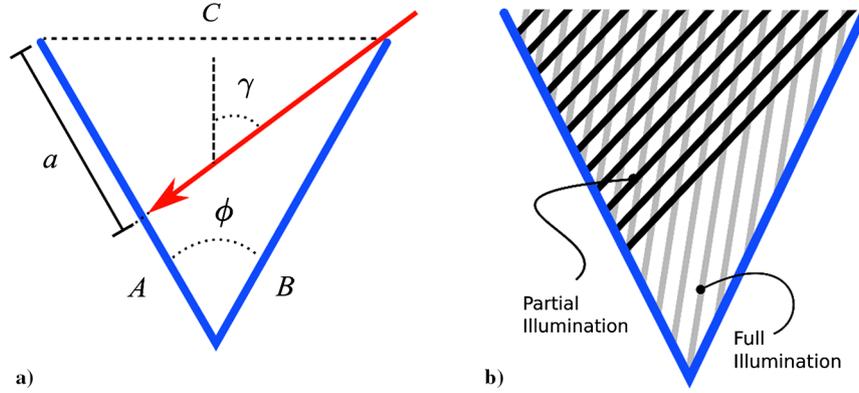$$\alpha_a = 1 - \frac{N_e}{N_t} \tag{2}$$

Fig. 1   Representations of a) V-groove cavity dimensions and nomenclature, and b) full or partial illumination.

To obtain the ratio N_e/N_t found in Eq. (1) or Eq. (2), a ray tracing program was created in Java following an algorithm as described in [24] with ray–plane collision equations found in [25]. Two scenarios were tested with this Java program to obtain the apparent emissivity/absorptivity of an infinite V-groove at a given cavity angle. First, a total of $N_t = 300{,}000$ rays were emitted diffusely from the cavity walls to determine the apparent emissivity for an isothermal cavity; this apparent emissivity was equivalent to the apparent absorptivity for a diffusely irradiated cavity as given by Ohwada's proof [26]. Second, a total of 150,000 collimated rays were emitted from the cavity opening into the cavity to determine the apparent absorptivity for collimated irradiation. The second test was performed at nine discrete values for γ, starting at zero and increasing by increments of $\pi/18$ rad (10 deg). Tests for both cases were performed over the entire range of cavity angles ϕ, from $\pi/180$ to $179\pi/180$ rad (1 to 179 deg) in increments of $\pi/180$ rad (1 deg). Tests were performed for 19 different intrinsic emissivity values (from 0.05 to 0.95 in increments of 0.05). Each combination of emissivity, cavity angle, and collimation angle was tested 20 times, and the average of the 20 tests was presented as the final result. The standard error of the mean ($SE = s/\sqrt{n}$ [27]) for each set of 20 tests was used as an estimate of the error of the ray tracing result. The total number of rays was selected such that the standard error of the mean for all tests remained below a value of 0.0005.

B.   Data Correlation

1.   Diffuse-Emission Apparent Emissivity Model and Diffuse-Irradiation Apparent Absorptivity Model

A radiative heat transfer model to predict the ratio N_e/N_t was developed by Psarouthakis [28] and is given in Eq. (3), where F is the view factor from one V-groove surface to the other. Because the view factor is $F = 1 - \sin(\phi/2)$, the model simplifies to Eq. (4) [16,29]:

$$\frac{q_e}{q_t} = \frac{N_e}{N_t} = (1 - F)[1 + F(1 - \varepsilon) + F^2(1 - \varepsilon)^2$$
$$+ F^3(1 - \varepsilon)^3 + \ldots + F^n(1 - \varepsilon)^n] \quad (3)$$

$$\frac{N_e}{N_t} = \sum_{n=0}^{\infty} (1 - \varepsilon)^n \left[1 - \sin\left(\frac{\phi}{2}\right)\right]^n \sin\left(\frac{\phi}{2}\right) \quad (4)$$

This model assumes that the radiosity from each wall is uniform. This assumption eliminates the integral equation found in Sparrow and Lin's model [10], but it introduces some error as the radiosity varies with position [30]. A correction function Λ_1 is introduced to offset the error introduced by the constant radiosity assumption. Substituting Eq. (4) and the correction function into Eq. (1) gives

$$\varepsilon_a = \alpha_a = \varepsilon \Lambda_1(\varepsilon, \phi) \sum_{n=0}^{\infty} (1 - \varepsilon)^n \left[1 - \sin\left(\frac{\phi}{2}\right)\right]^n \quad (5)$$

2.   Fully Illuminated Apparent Absorptivity Model ($\gamma \leq \phi/2$)

The nature of collimated irradiation is such that models for two separate scenarios must be developed. In the first scenario of $\gamma \leq \phi/2$, the collimated radiation is incident on both surfaces (Fig. 1b). In this case, the derivation of the diffuse-radiosity model is nearly identical to that of Psarouthakis [28], although an additional reflection must be included because energy is entering the cavity as opposed to being emitted from the cavity walls [Eq. (6)]:

$$\frac{N_e}{N_t} = \sum_{n=0}^{\infty} (1 - \varepsilon)^{n+1} \left[1 - \sin\left(\frac{\phi}{2}\right)\right]^n \sin\left(\frac{\phi}{2}\right) \quad (6)$$

Substituting Eq. (6) into Eq. (2) and introducing a correction factor Λ_2 to account for nonuniform radiosity, the apparent absorptivity of a fully illuminated V-groove exposed to collimated irradiation ($\gamma \leq \phi/2$) is given by

$$\alpha_a = 1 - \Lambda_2(\alpha, \phi, \gamma) \sum_{n=0}^{\infty} (1 - \alpha)^{n+1} \left[1 - \sin\left(\frac{\phi}{2}\right)\right]^n \sin\left(\frac{\phi}{2}\right) \quad (7)$$

3.   Partially Illuminated Apparent Absorptivity Model (γ is Greater than $\phi/2$)

When $\gamma > \phi/2$, then collimated radiation is incident only on a portion of one side of the V-groove as illustrated in Fig. 1b. The ratio N_e/N_t may again be determined using Psarouthakis's uniform radiosity approach [28], although partial illumination must now be considered. The number of rays that exit the cavity N_e is modeled by summing the percentage of rays that exit (reflectivity multiplied by view factor from the surface to the opening) after each successive reflection. The first four terms in this summation are given in Eq. (8), where the terms a, A, B, and C are illustrated in Fig. 1a:

$$N_e = N_t \rho F_{a-C} + N_t \rho F_{a-B} \rho F_{B-C} + N_t \rho F_{a-B} \rho F_{B-A} \rho F_{A-C}$$
$$+ N_t \rho F_{a-B} \rho F_{B-A} \rho F_{A-B} \rho F_{B-C} + \ldots \quad (8)$$

By including an infinite number of internal reflections, the ratio of the number of rays escaping the cavity to the total number of rays incident on the cavity opening is given by Eq. (9). The view factors F_{A-B} and F_{B-A} appearing in Eq. (8) are identical by symmetry. Likewise, the view factors F_{A-C} and F_{B-C} are identical by symmetry:

$$\frac{N_e}{N_t} = \rho F_{a-C} + \sum_{n=2}^{\infty} \rho^n F_{a-B} F_{B-C} F_{A-B}^{n-2} \quad (9)$$

The view factor F_{a-C} is determined using Hottel's crossed-strings method [29] [Eq. (10)], and $F_{a-B} = 1 - F_{a-C}$ is obtained from the summation rule:

$$F_{a-C} = \frac{1}{2}\left[1 + \sin\left(\frac{\phi}{2}\right) + \cos\left(\frac{\phi}{2}\right)\tan(\gamma) - \frac{\cos(\phi/2)}{\cos(\gamma)}\right] \quad (10)$$

A third correction function Λ_3 is introduced to offset errors due to the uniform radiosity assumption. Combining Eqs. (9) and (10) with Eq. (2) gives an expression for the apparent absorptivity when a V-groove is exposed to collimated irradiation with $\gamma > \phi/2$:

$$\alpha_a = 1 - \Lambda_3(\varepsilon, \phi, \gamma)\left[(1-\varepsilon)F_{a-C}\right.$$
$$\left. + \sum_{n=2}^{\infty}(1-\varepsilon)^n(1-F_{a-C})\sin\left(\frac{\phi}{2}\right)\left(1-\sin\left(\frac{\phi}{2}\right)\right)^{n-2}\right] \quad (11)$$

III.   Correction Function Results and Discussion

A.   Correlations

Correction functions were determined as functions of the intrinsic surface property (α or ε), geometry ϕ, and irradiation condition γ by correlating Eq. (5), (7), or (11) with ray tracing results. The Levenberg–Marquardt algorithm [31,32] was used to fit exponential basis functions to approximately 10,000 discrete data points and obtain the following expressions for Λ_1, Λ_2, and Λ_3. Table 1 provides a summary of the final correlations, giving the desired output, necessary inputs, limiting conditions imposed on the correlation, and necessary equation numbers, with all angles used in the equations (ϕ, γ) to be entered as radians.

1.   Diffuse-Emission Apparent Emissivity and Diffuse-Irradiation Apparent Absorptivity Model

The correction function needed to calculate the apparent emissivity or apparent absorptivity for diffuse irradiation using Eq. (5) is given by Eq. (12):

$$\Lambda_1(\varepsilon, \phi) = 1 - (0.0169 - 0.1900\,\ell n(\varepsilon))\exp(-1.4892\varepsilon^{-0.4040}\phi)$$
$$(12)$$

2.   Collimated Irradiation Apparent Absorptivity

The correction function needed to calculate the apparent absorptivity of a fully illuminated V-groove exposed to collimated irradiation ($\gamma \leq \phi/2$) using Eq. (7) is given by Eq. (13):

$$\Lambda_2(\alpha, \phi) = 1 - (0.0169 - 0.1900\,\ell n(\alpha))\exp(-1.4415\alpha^{-0.4240}\phi)$$
$$(13)$$

The correction function needed to calculate the apparent absorptivity of a partially illuminated V-groove exposed to collimated irradiation ($\gamma > \phi/2$) using Eq. (11) is given by Eqs. (14–17):

$$\Lambda_3(\alpha, \phi, \gamma) = D - E\exp(G\phi) \quad (14)$$

$$D = 0.0345\gamma^{-1.1447}\alpha^2 - 0.0414\gamma^{-0.8573}\alpha + 1$$
$$- 1.7702\exp(-18.0990\gamma) \quad (15)$$

$$E = -3.2301\exp(-1.1420\gamma)\exp(-2.6635\gamma^{-0.0370}\alpha) \quad (16)$$

$$G = -2.2780\gamma^{-0.5690}\alpha^{(0.1330\gamma^2 - 0.2372\gamma - 0.5434)} \quad (17)$$

B.   Apparent Radiative Property Behavior

With the correlations fully defined, the general behavior of the apparent emissivity and apparent absorptivity may be investigated and the effect of each parameter described.

1.   Apparent Emissivity

Figure 2a depicts the results of Eqs. (5) and (12) for the apparent emissivity of an isothermal, infinite V-groove as a function of cavity angle for intrinsic emissivity values of 0.05, 0.2, 0.4, and 0.6. When the surface is flat ($\phi = \pi$), the apparent emissivity is equal the intrinsic emissivity value, as expected. As the surface collapses and the cavity depth increases, the apparent emissivity increases monotonically. However, unlike the case of specular reflection [18], the apparent emissivity does not approach a value of unity as the V-groove collapses: a phenomenon that has been reported previously [33].

The ability to control the apparent emissivity and affect net radiation heat exchange between the surface and its surroundings is greater when the intrinsic emissivity is low. As an example, the apparent emissivity of a surface with an intrinsic emissivity of 0.05 may be increased by more than 800% to a value of 0.41 by decreasing the cavity angle. However, a V-groove with an intrinsic emissivity of 0.6 only increases by 50% to 0.9 with decreasing cavity angle.

2.   Apparent Absorptivity

The apparent absorptivity for a diffusely irradiated cavity is equivalent to the apparent emissivity of an isothermal cavity, as shown by Ohwada [26], and is given by Eqs. (5) and (12), with behavior as shown in Fig. 2a. The apparent absorptivity for a cavity with collimated irradiation entering normal to the cavity opening is shown in Fig. 3a for three intrinsic absorptivities. Because the V-groove is fully illuminated in the case of normal, collimated irradiation, Fig. 3a indicates the behavior of only the full-illumination correlation [Eqs. (7) and (13)]. Figure 3b displays apparent absorptivity as a function of cavity angle for collimation angles of $2\pi/9$ rad (20 deg) and $7\pi/9$ rad (70 deg) with intrinsic absorptivities of 0.1 and 0.6. For these offnormal conditions, the behavior of both the full [$\phi/2 \geq \gamma$, Eqs. (7) and (13)] and partial-illumination correlations [$\phi/2 < \gamma$, Eqs. (11) and (14–17)] are shown in Fig. 3b.

The collimation angle has a significant effect on the apparent absorptivity of the V-groove. When the collimated irradiation is normal to the surface ($\gamma = 0$), the apparent absorptivity approaches unity as the V-groove collapses, regardless of the intrinsic absorptivity, as shown in Fig. 3a. Note that this behavior differs from that observed for apparent emissivity. Furthermore, the apparent absorptivity is not equal to the apparent emissivity when a V-groove with diffuse and gray intrinsic surface properties are exposed to collimated irradiation. As shown in Fig. 3b, the apparent absorptivity decreases as the collimation angle increases, regardless of intrinsic absorptivity. This result is consistent with the fact that the projected area of the V-groove opening decreases as the collimation angle increases, which results in less radiation entering the cavity and less absorption. Furthermore, the apparent absorptivity approaches a value less than unity because the cavity angle collapses when the collimated irradiation is offnormal. This behavior highlights the fact that absorption by a diffusely reflecting V-groove depends strongly on the direction of collimated irradiation [12,14,18].

Table 1   Correlation summary for isothermal, diffusely reflecting V-grooves

| Desired output	Conditions	Required inputs	Equation numbers	Average relative error [standard deviation]	Maximum relative error
ε_a	Isothermal and diffuse emission with diffuse reflection	ε, ϕ	(5), (12)	0.3% [0.1%]	1.3%
α_a	Diffuse irradiation with diffuse reflection	α, ϕ	(5), (12)	0.3% [0.1%]	1.3%
α_a	Collimated, fully illuminated ($\gamma < \pi/2$) irradiation with diffuse reflection	α, γ, ϕ	(7), (13)	0.2% [0.2%]	0.6%
α_a	Collimated, partially illuminated ($\gamma > \pi/2$) irradiation with diffuse reflection	α, ϕ, γ	(11), (14–17)	2.0% [1.2%]	6.0%
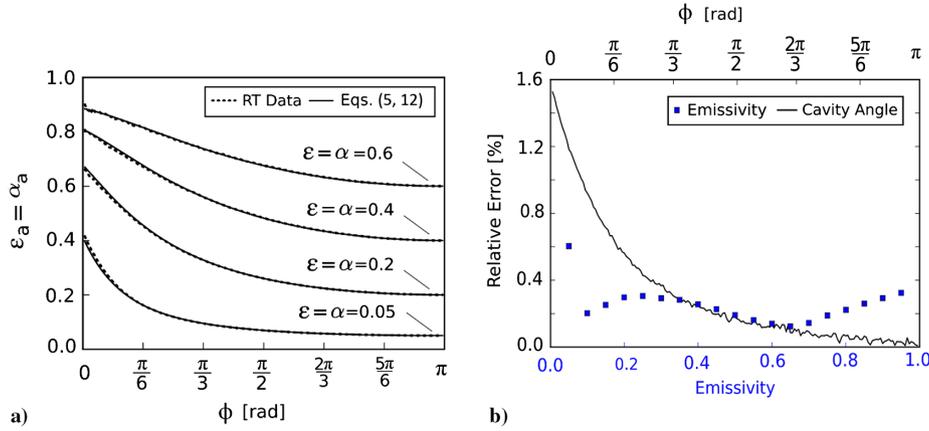
Fig. 2   Representations of a) apparent emissivity/absorptivity for diffuse irradiation and b) correlation relative error.
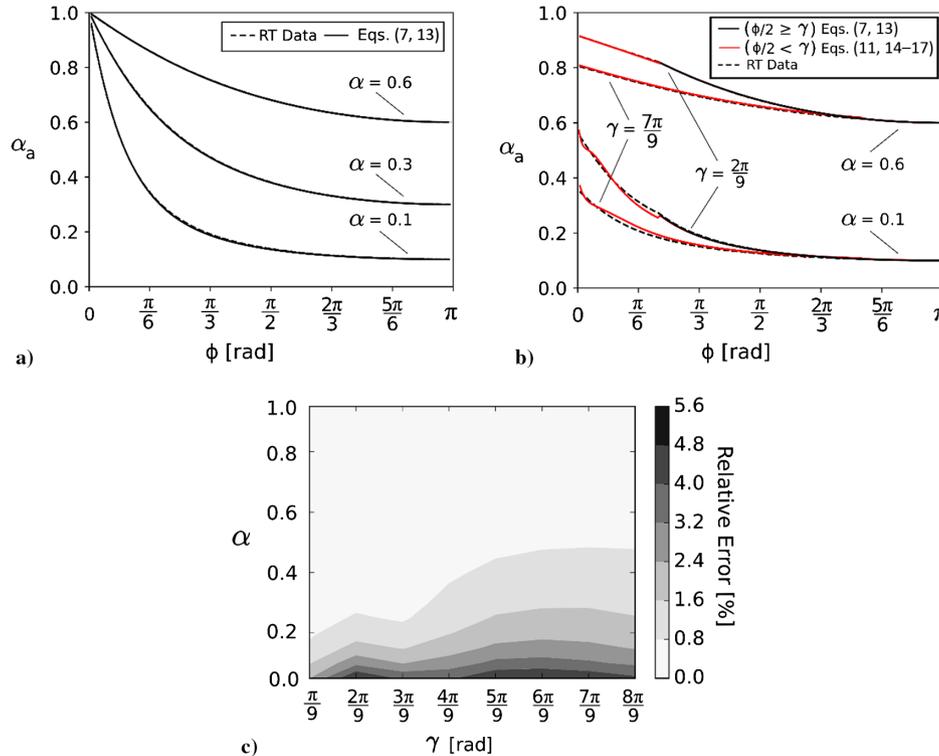

Fig. 3   Apparent absorptivity for a,b) full and b) partial illuminations; and c) relative error for partial illumination averaged over cavity angle.

C.   Comparison and Error Analysis

The accuracy of each correlation is assessed by comparison with the ray tracing (RT) data from which it is derived. The agreement between the correlation and RT data is excellent for the apparent emissivity correlation with an average relative error of 0.3% and a standard deviation of 0.1%, having a maximum relative error of 1.5%. Figure 2b illustrates the relative error between the RT data and the apparent emissivity correlation as a function of intrinsic emissivity, illustrating that the correlation is least accurate at the extreme values of intrinsic emissivity. The relative error as a function of cavity angle for an intrinsic emissivity of 0.95 is also shown in Fig. 2b. As the correlation is least accurate for large intrinsic emissivities, this curve represents the upper bound of the relative error as a function of cavity angle. Note that the accuracy of Eqs. (5) and (12) decreases as the cavity angle decreases. Results for the apparent emissivity are equivalent to the apparent absorptivity of a V-groove with diffuse reflection experiencing diffuse irradiation.

Figures 3a and 3b provide a comparison of RT data and correlation results for the case of full illumination. The correlation [Eqs. (7) and (13)] and RT data show excellent agreement, with an average relative error of 0.2% and a standard deviation of 0.23%, having a maximum relative error of 0.6%. The RT data and correlation results for partial illumination [Eqs. (11) and (14–17)] are shown in Fig. 3b for the case of $\phi/2 < \gamma$. As compared to the full-illumination correlation, the partial-illumination correlation is less accurate, with an average relative error of 2% and a standard deviation of 1.2%, having a maximum relative error of 6.0%. Figure 3c displays the relative error of the partial-illumination correlation with respect to ray tracing results, averaged over the cavity angle, as a function of the collimation angle and intrinsic absorptivity. The partial-illumination correlation [Eqs. (11) and (14–17)] is least accurate for low intrinsic absorptivities and large collimation angles, with the largest errors occurring for very small cavity angles ($\phi < \pi/6$).

To determine overall accuracy, the correlations and RT data were compared against analytical results digitally extracted from plots available in [10]. The correlation results agreed well with previously published analytical results, with only slight differences apparent for small cavity angles and small intrinsic absorptivity. Where a discrepancy existed between the analytical prediction and correlation, the RT results favored the analytical prediction. Overall,

the average relative error between the analytical models and all correlation results was 0.5%.

IV. Conclusions

The correlations provided in this work (Table 1) provide a simple, accurate, and rapid method of apparent radiative property calculation for the infinite V-groove exposed to diffuse or collimated irradiation. The average value of the relative error for all correlations proposed in this work as compared to the ray tracing data is less than 2.0%, with the maximum never exceeding 6.0%. When compared with analytical models, the average error of the correlations is 0.5%. The least accurate predictions occur for small cavity angles, intrinsic absorptivities, and collimation angles.

Acknowledgments

References

[1] Blanc, M. J., Mulford, R. B., Jones, M. R., and Iverson, B. D., "Infrared Visualization of the Cavity Effect Using Origami-Inspired Surfaces," *Journal of Heat Transfer*, Vol. 138, No. 2, 2016, Paper 020901.
doi:10.1115/1.4032229

[2] Mulford, R. B., Jones, M. R., and Iverson, B. D., "Dynamic Control of Radiative Surface Properties with Origami-Inspired Design," *Journal of Heat Transfer*, Vol. 138, No. 3, 2015, Paper 032701.
doi:10.1115/1.4031749

[3] Iverson, B. D., Mulford, R. B., Lee, E. T., and Jones, M. R., "Adaptive Net Radiative Heat Transfer and Thermal Management with Origami-Structured Surfaces," *16th International Heat Transfer Conference*, Heat & Mass Transfer Soc. of China Paper IHTC16-23600, Beijing, Aug. 2018.

[4] Lang, F., Wang, H., Zhang, S., Liu, J., and Yan, H., "Review on Variable Emissivity Materials and Devices Based on Smart Chromism," *International Journal of Thermophysics*, Vol. 39, 2018, p. 6.
doi:10.1007/s10765-017-2329-0

[5] Liu, Y., Qiu, J., Zhao, J., and Liu, L., "General Design Method of Ultra-Broadband Perfect Absorbers Based on Magnetic Polaritons," *Optics Express*, Vol. 25, No. 20, 2017, pp. A980–A989.
doi:10.1364/OE.25.00A980

[6] Sergeant, N. P., Agrawal, M., and Peumans, P., "High Performance Solar Selective Absorbers Using Coated Sub Wavelength Gratings," *Optics Express*, Vol. 18, No. 6, 2010, pp. 5525–5540.
doi:10.1364/OE.18.005525

[7] Huang, Z., and Ruan, X., "Nanoparticle Embedded Double-Layer Coating for Daytime Radiative Cooling," *International Journal of Heat and Mass Transfer*, Vol. 104, Jan. 2017, pp. 890–896.
doi:10.1016/j.ijheatmasstransfer.2016.08.009

[8] Vall, S., and Castell, A., "Radiative Cooling as Low-Grade Energy Source: A Literature Review," *Renewable and Sustainable Energy Reviews*, Vol. 77, Sept. 2017, pp. 803–820.
doi:10.1016/j.rser.2017.04.010

[9] Benkahoul, M., Chaker, M., Margot, J., Haddad, E., Kruzelecky, R., Wong, B., Jamroz, W., and Poinas, P., "Thermochromic VO2 Film Deposited on Al with Tunable Thermal Emissivity for Space Applications," *Solar Energy Materials and Solar Cells*, Vol. 95, No. 12, 2011, pp. 3504–3508.
doi:10.1016/j.solmat.2011.08.014

[10] Sparrow, E. M., and Lin, S. H., "Absorption of Thermal Radiation in a V-Groove Cavity," *International Journal of Heat and Mass Transfer*, Vol. 5, No. 11, 1962, pp. 1111–1115.
doi:10.1016/0017-9310(62)90064-9

[11] Sparrow, E. M., and Lin, S. H., "Radiation Heat Transfer at a Surface Having Both Specular and Diffuse Reflectance Components," *International Journal of Heat and Mass Transfer*, Vol. 8, No. 5, 1965, pp. 769–779.
doi:10.1016/0017-9310(65)90023-2

[12] Zipin, R. B., "The Directional Spectral Reflectance of Well Characterized Symmetric V Grooved Surfaces," Ph.D., Purdue Univ., West Lafayette, IN, 1965.

[13] Zipin, R. B., "The Apparent Thermal Radiation Properties of an Isothermal V-Groove with Specularly Reflecting Walls," *Journal of Research of the National Bureau of Standards*, Vol. 70c, No. 4, 1966, pp. 275–280.
doi:10.6028/jres.070C.026

[14] Black, W. Z., "Optimization of Directional Emission from V-Groove and Rectangular Cavities," *Journal of Heat Transfer*, Vol. 95, No. 1, 1973, pp. 31–36.
doi:10.1115/1.3450000

[15] Black, W. Z., and Schoenhals, R. J., "A Study of Directional Radiation Properties of Specially Prepared V-Groove Cavities," *Journal of Heat Transfer*, Vol. 90, No. 4, 1968, pp. 420–428.
doi:10.1115/1.3597537

[16] Modest, M. F., *Radiative Heat Transfer*, Academic Press, New York, 2013, pp. 211–212.

[17] Hollands, K. G. T., "Directional Selectivity, Emittance, and Absorptance Properties of Vee Corrugated Specular Surfaces," *Solar Energy*, Vol. 7, No. 3, 1963, pp. 108–116.
doi:10.1016/0038-092X(63)90036-7

[18] Mulford, R. B., Collins, N. S., Farnsworth, M. S., Jones, M. R., and Iverson, B. D., "Total Hemispherical Apparent Radiative Properties of the Infinite V-Groove with Specular Reflection," *International Journal of Heat and Mass Transfer*, Vol. 124, Sept. 2018, pp. 168–176.
doi:10.1016/j.ijheatmasstransfer.2018.03.041

[19] Yang, Y., and Wang, L., "Spectrally Enhancing Near-Field Radiative Transfer Between Metallic Gratings by Exciting Magnetic Polaritons in Nanometric Vacuum Gaps," *Physical Review Letters*, Vol. 117, No. 4, 2016, Paper 044301.
doi:10.1103/PhysRevLett.117.044301

[20] Sapritsky, V. I., and Prokhorov, A. V., "Calculation of the Effective Emissivities of Specular Diffuse Cavities by the Monte Carlo Method," *Metrologia*, Vol. 29, No. 1, 1992, pp. 9–14.
doi:10.1088/0026-1394/29/1/003

[21] Prokhorov, A. V., "Monte Carlo Method in Optical Radiometry," *Metrologia*, Vol. 35, No. 4, 1998, pp. 465–471.
doi:10.1088/0026-1394/35/4/44

[22] Prokhorov, A. V., Hanssen, L. M., and Mekhontsev, S. N., "Calculation of the Radiation Characteristics of Blackbody Radiation Sources," *Experimental Methods in the Physical Sciences*, Vol. 42, 2009, pp. 181–240.
doi:10.1016/S1079-4042(09)04205-2

[23] Tang, K., Dimmena, R. A., and Buckius, R. O., "Regions of Validity of the Geometric Optics Approximation for Angular Scattering from Very Rough Surfaces," *International Journal of Heat and Mass Transfer*, Vol. 40, No. 1, 1996, pp. 49–59.
doi:10.1016/S0017-9310(96)00073-7

[24] Steinfeld, A., "Apparent Absorptance for Diffusely and Specularly Reflecting Spherical Cavities," *International Journal of Heat and Mass Transfer*, Vol. 34, No. 7, 1990, pp. 1895–1897.
doi:10.1016/0017-9310(91)90163-9

[25] Foley, J., van Dam, A., Feiner, S., and Hughes, J., "Clipping Lines," *Computer Graphics*, Addison-Wesley Professional, Boston, MA, 2013.

[26] Ohwada, Y., "Mathematical Proof of an Extended Kirchhoff Law for a Cavity Having Direction-Dependent Characteristics," *Journal of the Optical Society of America*, Vol. 5, No. 1, 1988, pp. 141–145.
doi:10.1364/JOSAA.5.000141

[27] Navidi, W., *Statistics for Engineers and Scientists*, McGraw-Hill, New York, 2010, p. 21.

[28] Psarouthakis, J., "Apparent Thermal Emissivity from Surfaces with Multiple V-Shaped Grooves," *AIAA Journal*, Vol. 1, No. 8, 1963, pp. 1879–1882.
doi:10.2514/3.1939

[29] Howell, J. R., Siegel, R., and Menguc, M. P., *Thermal Radiation Heat Transfer*, CRC Press, Boca Raton, FL, 2011.

[30] Sparrow, E. M., Gregg, J. L., Svel, J. V., and Manos, P., "Analysis, Results and Interpretation for Radiation Between Some Simply-Arranged Gray Surfaces," *Journal of Heat Transfer*, Vol. 83, No. 2, 1961, pp. 207–214.
doi:10.1115/1.3680523

[31] More, J. J., "The Levenberg-Marquardt Algorithm: Implementation and Theory," *Numerical Analysis*, Vol. 630, Lecture Notes in Mathematics, edited by G. A. Watson, Springer, Berlin, 1978.

[32] Oliphant, T. E., "Python for Scientific Computing," *Computing in Science and Engineering*, Vol. 9, No. 3, 2007, pp. 10–20.
doi:10.1109/MCSE.2007.58

[33] Sparrow, E. M., "Radiant Emission Absorption and Transmission Characteristics of Cavities and Passages," NASA Special Rept. NASA SP-55/19650017263, 1965, pp. 103–115.